Vol. 80: 223–242, 2017
https://doi.org/10.3354/ame01854

AQUATIC MICROBIAL ECOLOGY
Aquat Microb Ecol

Published online November 24

Winter mixing impacts gene expression in marine microbial populations in the Gulf of Aqaba

D. Miller[1], U. Pfreundt[2,3], S. Hou[2], S. C. Lott[2], W. R. Hess[2], I. Berman-Frank[1,*]

[1]Mina and Everard Goodman Faculty of Life Sciences, Bar Ilan University, Ramat Gan, Israel
[2]Genetics and Experimental Bioinformatics, Faculty of Biology, University of Freiburg, Schänzlestr. 1, 79104 Freiburg, Germany

[3]*Present address:* ETH Zürich, Department of Civil, Environmental and Geomatic Engineering, Institute of Environmental Engineering, Stefano-Franscini-Platz 5, 8093 Zürich, Switzerland

ABSTRACT: In aquatic systems, changes in temperature and irradiance fundamentally characterize the water column and regulate microbial population structure and function. In systems with stable thermal stratification, the warm surface mixed layer is typically nutrient impoverished, limiting biological production. In periods of destratification, convective mixing of the water column exposes the microorganisms inhabiting these mixed systems to rapid variations in light availability and spectra. We explored the impact of winter deep-mixing (500 m deep mixed layer) on microbial communities from the surface (2.5 m) and the aphotic waters (440 m) in the Gulf of Aqaba by examining changes in both population composition and function via DNA and RNA sequencing. The greatest fraction of 16S sequences was assigned to *Euryarchaeota*, while metatranscriptomes were dominated by *Synechococcus* transcripts. Community composition was highly similar at both depths, yet transcription profiles differed. Phototrophic organisms found at the photic surface overexpressed genes related to catabolism and energy metabolism, while genes affiliated with biosynthesis were overexpressed at the aphotic depth. Similar transcriptional trends were observed in the non-photoautotrophs SAR11, *Euryarchaeota*, and *Thaumarchaeota*, with niche partitioning based on differential utilization of nitrogen and phosphorus occurring between the 2 archaeal groups. We did not detect upregulated expression of cyanobacterial genes indicative of mixotrophy or glycogen metabolism in the aphotic zone, suggesting they survive the aphotic period by utilizing photosynthates produced in the photic zone. Indications for a mixotrophic lifestyle were observed for prasinophytes, with genes related to phagocytosis overexpressed at the aphotic depth compared with the surface.

KEY WORDS: Deep mixing · Red Sea · Metatranscriptomics · Cyanobacteria · SAR11 · *Archaea* · Prasinophytes

INTRODUCTION

Irradiance is a primary driver of phototroph distribution and physiology in aquatic systems, where the exponential decay of light intensity and changing spectra define a gradient of environments and create photic and aphotic zones. Seasonal thermal stratification and destratification cycles further impact the vertical distribution of microbial organisms throughout the water column. In fully stratified systems, planktonic microbial cells may be exposed regularly to diel light cycles or inhabit the aphotic (dark) zone. In seasonally mixed water columns, cells are often driven across the photic boundary by vertical mixing. In these dynamic environments, planktonic microorganisms develop strategies that allow their survival in a rapidly changing environment with varying light conditions. Several studies have assessed the differences in microbial community composition and functionality between different layers of the water col-

*Corresponding author: ilana.berman-frank@biu.ac.il

Publisher: Inter-Research · www.int-res.com

umn (Ghiglione et al. 2007, 2008, Tamburini et al. 2009, Korlević et al. 2015). In metagenomic surveys from oligotrophic stratified environments, including the northwest Pacific Ocean and the Sargasso, Mediterranean, and Red Seas, *Prochlorococcus*, *Verrucomicrobiales*, *Flexibacteraceae*, *Euryarchaeota*, and *Gamma-*, *Delta-*, and *Alphaproteobaceria* dominated surface-water microbial populations (DeLong et al. 2006, Ferreira et al. 2014, Thompson et al. 2017). The dominant metabolic pathways in surface waters (based on sequence similarity searches of metagenome sequences against protein data bases) included chlorophyll and carotenoid biosynthesis, carbon fixation, light-induced DNA repair, oxidative stress responses, nitrogen and phosphate metabolism, and vitamin B6 metabolism (DeLong et al. 2006, Ferreira et al. 2014, Thompson et al. 2017). At aphotic depths, representatives from *Deferribacteres*, *Planctomycetaceae*, *Acidobacteriales*, *Gemmatamonadaceae*, *Nitrospina*, *Alteromonadaeceae*, and *Thaumarchaeota* prevailed (DeLong et al. 2006, Ferreira et al. 2014), while characteristic metabolic functions included protein folding and export, glyoxylate and dicarboxylate metabolism, thiamine metabolism, methane oxidation, selenocysteine metabolism and terpenoid biosynthesis, and sulfate assimilation and metabolism (DeLong et al. 2006, Ferreira et al. 2014). Hence, taxonomic and functional profiles characterizing certain depths can be established from nucleic acid sequencing assays. However, vertical mixing can modify these characteristic profiles, as described from the Humboldt Current upwelling system along the Chilean coastline (Ferreira et al. 2014).

The restricted influx of cold water over a shallow southern sill produces high minimal temperatures (~20.6°C) throughout the water column of the northern Gulf of Aqaba, Red Sea (Reiss & Hottinger 1984). During summer stratification, typical surface temperatures reach 28°C and the mixed layer depth is <30 m. With declining fall–winter air temperatures, the upper layer cools and sinks, causing destratification, and mixing may typically reach 300–400 m by late February/early March and can deepen to ~800 m during extremely cold winters (Wolf-Vecht et al. 1992, Genin et al. 1995, Carlson et al. 2014).

This deep mixing results in a fairly uniform distribution of the picoplanktonic populations of *Prochlorococcus*, *Synechococcus*, and unicellular eukaryotic algae within the mixed water column, including the aphotic depths (Lindell & Post 1995). Here, we examined the microbial population structure and function from a photic and aphotic depth in the northern Gulf of Aqaba during winter deep mixing that reached 500 m depth. We assessed and analyzed the contribution of taxonomic groups within the microbial community from photic and aphotic depths by 16S gene sequencing. Concurrently, we analyzed microbial transcriptional activity using metatranscriptomics. To capture genes that are expressed as a response to changes associated with convection, we assessed only nascent (recently transcribed) transcripts using meta-differential RNA-seq (mdRNA-seq, Hou et al. 2016). We further analyzed the data examining the ecophysiological implications for representative species from abundant taxa, including photoautotrophic cyanobacteria, photoheterotrophic bacteria (SAR11), archaea, and picoeukaryotic algae.

MATERIALS AND METHODS

Sampling procedures and site

Samples were collected on 5 February 2012 at Stn A in the Gulf of Aqaba (29° 28′ N, 34° 55′ E, ~700 m bottom depth) from 2 depths at 09:45 h (2.5 and 440 m) and from 45 m at 14:45 h (GMT +2). The sample collected in the afternoon was obtained in the framework of a different project aiming to compare dRNA-seq (see below) with standard RNA-seq (Hou et al. 2016). We also used the 45 m sample for the investigation of 16S-based community composition and taxonomic assignment of RNA reads (see Fig. 2). Water samples were obtained using a rosette device equipped with 12 Niskin bottles of 10 l each and CTD sensors detecting temperature, salinity, chlorophyll *a* (chl *a*)-induced fluorescence, oxygen, and photosynthetically active radiation (PAR). For each RNA sample, 10 l of water were collected from each of 4 Niskin bottles and immediately filtered in a shaded area onboard through a 20 µm mesh onto polyethersulfone filters (PALL Supor, 47 mm diameter, 0.45 µm pore size). Minimal volume filtered was 2.6 l and maximal volume reached approximately 5 l. Filtration time did not exceed 20 min to minimize filtration stress and expression of genes resulting from filtration and environmental shift. The duration of the deepest cast was approximately 30 min from the deepest point (~700 m) to the surface, and ~20 min were required for the 440 m sample to reach the deck. Filters were subsequently placed in 1 ml of RNA resuspension buffer (10 mM NaOAc pH 5.2, 200 mM D (+)-sucrose, 100 mM NaCl, 5 mM EDTA), immediately frozen in liquid nitrogen, and kept at –80°C until further analysis. RNA extraction and library preparation was performed according to the

mdRNA-seq approach (Sharma et al. 2010, Hou et al. 2016). The procedure is described below and detailed in Supplement 1 at www.int-res.com/articles/suppl/a080p223_supp1.pdf.

Inorganic nutrient measurements

Seawater for inorganic nutrient analyses (orthophosphate, nitrate, and nitrite) was collected in acid-washed plastic 20 ml vials. Samples were immediately frozen and thawed upon analysis. Nutrient concentrations were determined colorimetrically using a flow injection autoanalyzer (FIA Lachat Instruments Model QuickChem 8000). Peak areas were calibrated using standards prepared with nutrient-depleted filtered sea water. Phosphate was preconcentrated by a factor of ~20 by applying the magnesium co-precipitation (MAGIC) protocol (Karl & Tien 1992). The precision of nitrate + nitrite and orthophosphate measurements was 0.05 and 0.02 µM, respectively.

Flow cytometry

Picophytoplankton cell abundance was determined using flow cytometry. Samples of 1.8 ml were fixed immediately after sampling with 5 µl of 50% glutaraldehyde (Sigma G-7651), incubated at room temperature for 10 min, frozen in liquid nitrogen, and kept at −80°C until further analysis. Prior to the analysis, fixed samples were gradually thawed in a 37°C water bath. Analysis was performed using a FACScan Attune, fitted with argon lasers (405 and 488 nm). Beads of 1 µm diameter (Polysciences) served as standards (Marie et al. 1997, Sosik et al. 2010). The taxonomic discrimination was based on cell side scatter (a proxy of cell volume), forward scatter (a proxy of cell size), and orange and red fluorescence of phycoerythrin and chl *a* (filters: 574/26 nm band pass and 640 nm long pass, respectively). Phytoplankton carbon (C) biomass was calculated from cell counts assuming 225 fg C cell^{-1} for *Synechococcus* cells, 60 fg C cell^{-1} for *Prochlorococcus* cells, and 1319 fg C cell^{-1} for picoeukaryotes (Buitenhuis et al. 2012).

DNA extraction and amplification of 16S rRNA gene sequences

Water samples (2 l) were filtered on 47 mm, 0.45 µm pore size Supor filters (Pall Gelman) and snap frozen in liquid nitrogen. The filters were kept at −80°C until DNA extraction, performed with phenol-chloroform using a modification of the protocols described by Brinkhoff & Muyzer (1997) and Massana et al. (1997). For amplicon sequencing, we used the primer pair S-D-Bact-0341-b-S-17/S-D-Bact-0785-a-A-21 (Klindworth et al. 2013), which targets the V3-V4 region of the 16S rRNA gene of bacteria and archaea. Amplicons were sequenced on a MiSeq Illumina™ sequencer in paired-end mode (300 bp × 2 per fragment).

RNA extraction and library preparation

The RNA sampling procedure was described elsewhere (Pfreundt et al. 2014). Briefly, sampled seawater was filtered onboard in a shaded working space directly upon retrieval of the rosette, for no longer than 20 min. Water samples were pre-filtered using a 20 µm mesh onto 0.45 µm pore size polyethersulfone filters (PALL Supor). Filters were immediately placed in 1 ml of RNA resuspension buffer (10 mM NaAc pH 5.2, 200 mM D(+) sucrose, 100 mM NaCl, 5 mM EDTA) and snap frozen in liquid nitrogen. Samples were kept at −80°C until further processing.

Total RNA was extracted using phenolic PGTX (modified from Pinto et al. 2009), DNAse treated (Ambion), and purified (Clean&Concentrator® columns Zymo Research). dRNA-seq libraries were prepared according to Sharma et al. (2010). RNA molecules carrying a 5′ monophosphate were degraded using Terminator exonuclease (Epicentre), and the 5′ sequencing adapter (including sample barcode) was ligated. This resulted in a library highly enriched in nascent transcripts. cDNA first-strand synthesis was performed using random hexameric primers followed by the ligation of a second PCR adapter at the original 3′ end of the RNA (now found at the 5′ end of the cDNA first strand). The resulting cDNA molecules were then PCR amplified using biotinylated 5′ primers, and PCR products were fragmented by sonication. Fragments of 300–500 bp were size-selected and attached to streptavidin beads, and the 3′ Illumina sequencing adapter was ligated. Bead-bound fragments were subjected to a second, short PCR amplification and sequenced on an Illumina Hi-Seq platform. This procedure resulted in a library of reads originating at the 5′ end of the transcripts present in the sample, allowing downstream analyses to determine the real transcription start site (TSS) of the transcript (see below).

All raw reads were uploaded to the NCBI Sequence Read Archive (SRA) under the BioProject accession number PRJNA248420.

Analysis of 16S gene sequence abundance and microbial population composition

The analysis pipeline of 16S amplicons was followed as described by Pfreundt et al. (2016b). Briefly, all steps of the bioinformatic analysis were performed using the USEARCH pipeline and the UPARSE package (Edgar 2013). Reads in fastq format were quality filtered and converted to fasta format before clustering 100% identical reads, discarding singletons, and defining operational taxonomic unit (OTU) clusters (maximum dissimilarity of 2%). Chimeras were auto-filtered by the OTU clustering algorithm. OTUs were mapped to the SILVA SSU database (release 119.1; https://www.arb-silva.de/). The threshold for classification was (% sequence identity + % sequence coverage) / 2 > 93%.

Bioinformatics analysis of metatranscriptomes

For a more detailed description of bioinformatics approaches, see Supplement 1.

The complete analysis pipeline of metatranscriptome libraries is visualized in Fig. S1 (all supplementary figures are available in Supplement 1). Following sequencing, raw reads were subjected to quality control, adapter trimming, and computational removal of rRNA reads. The obtained sequences were subjected to similarity searches against the NCBI nt database (downloaded in March 2016 from ftp://ftp.ncbi.nlm.nih.gov/blast/db/) using LAST (Kiełbasa et al. 2011). The LAST search was performed with default parameters using the 'BlastTab+' output option except for the following switches: -K 10 and -N 25 (see LAST documentation for further details). The taxonomic affiliations of transcriptome reads were analyzed using MEGAN 5.

We used reference genomes obtained from the RefSeq database (Tatusova et al. 2014) instead of a self-assembled reference. A former approach trying to de novo assemble the metatranscriptomes into transcripts and use them as references did not yield satisfactory results (Pfreundt et al. 2014). This was likely due to the fact that dRNA-seq enriches the sequence library with reads assigned to the 5′ end of transcripts, restricting the distribution of reads over the full transcript length. In addition, concerns have been raised in the past regarding the assembly of reads emerging from complex communities of metagenomes and metatranscriptomes (Charuvaka & Rangwala 2011, Mende et al. 2012).

Reference genomes were identified for each taxonomic group separately. For cyanobacteria, the majority of reads were mapped to the *Synechococcus* CC9605 genome (21 and 44% for 2.5 and 440 m). In the case of SAR11, the 3 complete genomes found in the RefSeq database were compared as references for all reads assigned to SAR11 using dc-megablast. *Pelagibacter* sp. HTCC7211 recruited the highest percentage of reads (38 and 43%) and was selected as a reference. No suitable reference genome could be found in RefSeq for *Euryarchaeota* or *Thaumarchaeota*. To generate a reference for mapping, archaeal reads were first mapped to a set of 997 archaeal contigs from a Mediterranean Sea metagenomics library (Deschamps et al. 2014). Contigs recruiting at least 200 reads were extracted and used as a reference. This resulted in a reference composed of 115 contigs ascribed to the *Euryarchaeota* MG-II/III and a second reference for *Thaumarchaeota*, composed of 107 contigs. These references recruited 56–95% of all archaeal reads. A separately defined set of MG-II/III genomic bins (Li et al. 2015) did not improve this recruitment. All annotations used were based on the original annotations of the 997 published contigs. The *Micromonas* sp. RCC299 genome, which recruited 74 and 71% of *Mamiellales* reads at 2.5 and 440 m, respectively, was selected as a representative of this group.

Expression levels were defined as the averaged forward and reverse read counts assigned to a transcript (coding sequences, non-coding RNA, rRNA, and tRNA genes) for which a TSS was detected (hereafter: TSS expression). In some cases, transcripts without a detected TSS but with a clearly high recruitment of reads were also considered in the final analysis.

Following mapping to reference genomes, TSSs were inferred as previously described (Hou et al. 2016) and outlined in Supplement 1. After detecting TSSs, averaged values of counts of forward and reverse reads assigned to each TSS were used as a measure for expression level of the associated gene. These values were compared between the different depths for differential expression (DE) analysis using NOISeq (Tarazona et al. 2011). The calculation of DE was based on trimmed mean of M (TMM)-normalized TSS expression values (Robinson & Oshlack 2010) using 5 technical repeat simulations, each representing 20% of complete sample size. Variability of 2% was presumed, and the probability threshold for DE was set to 0.9. Transcripts with <2 counts per million were excluded from the analysis. Since the length of each examined feature (transcript) is known from the reference genome, length correction was also included in the analysis. In some cases, 2

different TSSs of the same gene were differentially expressed, indicating possibly alternatively regulated promoters. Since no data were available on the different functions of such hypothetical transcripts, they were treated as synonymous and were considered as differentially expressed when the TMM value of an overexpressed transcript in one sample was at least 3-fold higher compared to the TMM value of the other transcript, detected as overexpressed in the other sample.

Protein sequences of all transcripts identified for each of the reference genomes were used for Blast-KOALA searches (Kanehisa et al. 2016) against the Kyoto Encyclopedia of Genes and Genomes (KEGG) database (Kanehisa & Goto 2000). The resulting KEGG-orthologs (KOs) were visualized using iPath2.0 (Yamada et al. 2011). The procedure was also performed on lists of differentially expressed KO numbers, and depth-specific functional profiles were generated in the form of heat maps visualizing the number of differentially expressed KOs recruited to KEGG pathways at each depth.

RESULTS AND DISCUSSION

Defining environmental conditions

Samples were collected on 5 February 2012 at Stn A in the northern Gulf of Aqaba (29° 28′ N, 34° 55′ E, bottom depth ~700 m), when vertical mixing reached a depth of 500 m. Depth profiles of temperature, salinity, dissolved oxygen, inorganic nutrients, and chl *a* concentrations were reported elsewhere (Pfreundt et al. 2014). Mixed-layer water temperature was ~21.3°C (with a minimal difference of 0.1°C between the surface and the aphotic samples). Salinity remained stable at 40.7 PSU from the surface to 500 m. The concentrations of inorganic nutrients ranged from 1.7–2.2 µmol l^{-1} NO_3 + NO_2 (hereafter total inorganic nitrogen, TIN), 0.99–1.08 µmol l^{-1} $Si(OH)_4$, and 0.1–0.12 µmol l^{-1} PO_4. Nutrient concentrations were higher than typical summer values, when surface concentrations decline to 0.05 µmol l^{-1} TIN, 0.8 µmol l^{-1} $Si(OH)_4$, and <0.01–0.02 µmol l^{-1} PO_4 (Mackey et al. 2007, Lazar et al. 2008, Meeder et al. 2012, Miller et al. 2017), emphasizing the seasonal variability in nutrient availability. The measured winter concentrations were nonetheless comparable to low dissolved inorganic nutrient concentrations measured from the upper surface layers in other oligotrophic locations (Karl et al. 1993, Dore et al. 1996). PAR declined with an absorption coefficient (K_d) of 0.058 m^{-1} from 1063 µmol quanta m^{-2} s^{-1} at the sea surface to 1 and 0.01% at 90 and 193 m, respectively (Fig. 1a). Chl *a* concentration of 0.1 µg l^{-1} was measured throughout the mixed layer and decreased below 500 m until it was no longer detectable at 567 m (Pfreundt et al. 2014), consistent with the mixed layer depth.

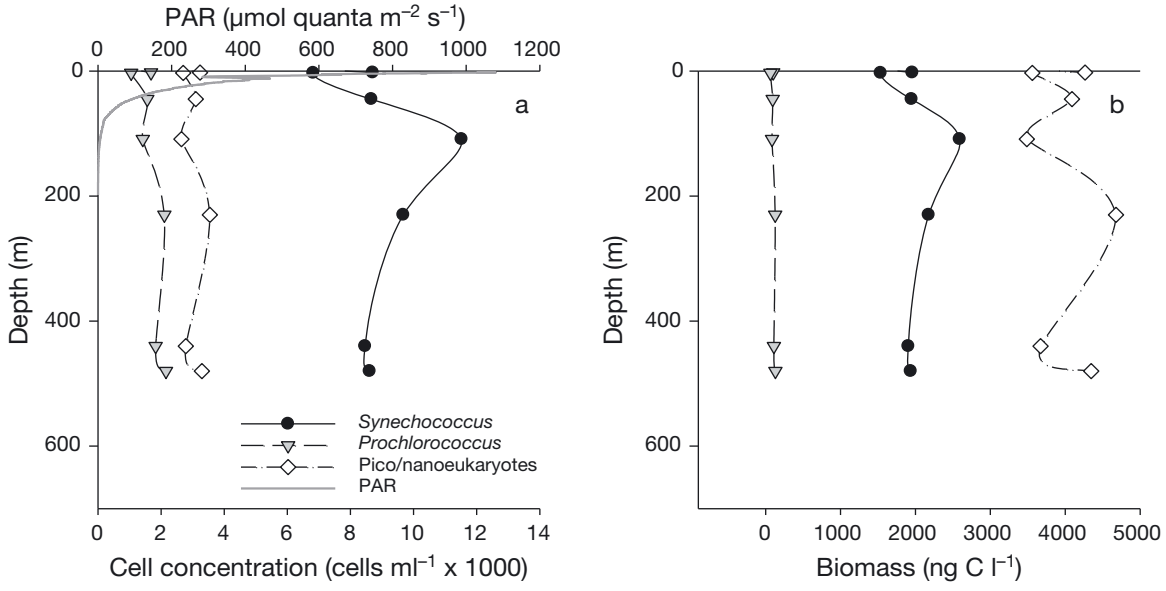

Fig. 1. Distribution of picoplanktonic groups collected on 5 February 2012 at Stn A in the northern Gulf of Aqaba. (a) Depth profiles of *Prochlorococcus, Synechococcus*, and picoeukaryotic algae cell concentrations based on flow cytometry measurements. Gray solid line shows the intensity of photosynthetically active radiation (PAR) as a function of depth. (b) Phytoplankton carbon biomass for the 3 groups calculated based on cell counts (see 'Materials and methods' for details)

Photoautotroph abundance

The predominant contributors to the picophytoplankton (*Synechococcus, Prochlorococcus,* and picoeukaryotic algae with a diameter of <3 µm) were distributed throughout the 500 m mixed layer (Fig. 1). Of the total picophytoplankton biomass, picoeukaryotic algae comprised 72.5–81.8% (3490–4680 ng C l^{-1}), followed by 17.2–26.3% assigned to *Synechococcus* (1534–2590 ng C l^{-1}) and 0.9–1.5% of the total biomass attributed to *Prochlorococcus* (63–130 ng C l^{-1}, Fig. 1b). Picoeukaryotes have an average diameter of 2–5 µm compared to the <1 µm of *Prochlorococcus* and ~1 µm of *Synechococcus* (Olson et al. 1990, Veldhuis & Kraay 1990). The capacity for luxury uptake and storage of the assimilated nutrients increases with larger cell size (Raven & Kübler 2002), providing the larger picoeukaryotes with a competitive advantage under higher nutrient concentrations (Kriest & Oschlies 2007). Therefore, increased nutrient availability caused by seasonal deep mixing enables picoeukaryotic algae to produce more biomass (Lindell & Post 1995, Mackey et al. 2007). Deep mixing also leads to the circulation of photosynthetic cells throughout the aphotic zone, with chl a_2, indicative of *Prochlorococcus*, found at aphotic depth during winter mixing (Lindell & Post 1995).

Our data show that while *Prochlorococcus* biomass comprised only 0.9–1.5% of total picoplankton biomass (Fig. 1), it was the 11th most abundant group within the total classified mRNA pool at 2.5 and 45 m, and the ninth most abundant at 440 m (contributing 0.2% in all 3 depths; Fig. 2b). *Synechococcus* contributed 18–19% of picophytoplankton biomass, but comprised a relatively low fraction of all 16S sequences (1.3, 1.4, and 2.5% at 2.5, 45 and 440 m, respectively; Fig. 2a and see below). Yet, the highest fraction of transcripts at the classified mRNA pool at all depths was attributed to this group (Fig. 2b). Active transcription demonstrates that cyanobacteria were present and transcriptionally active throughout the mixed layer, including the aphotic zone. If present for prolonged periods, they could potentially provide an inoculum for rapid growth in the summer, when environmental conditions favor the development of small cells with a large surface area to volume ratio enabling efficient uptake rates.

Population composition and transcriptional activity

Sequencing of 16S rRNA genes yielded similar (but not identical) composition of microbial populations at

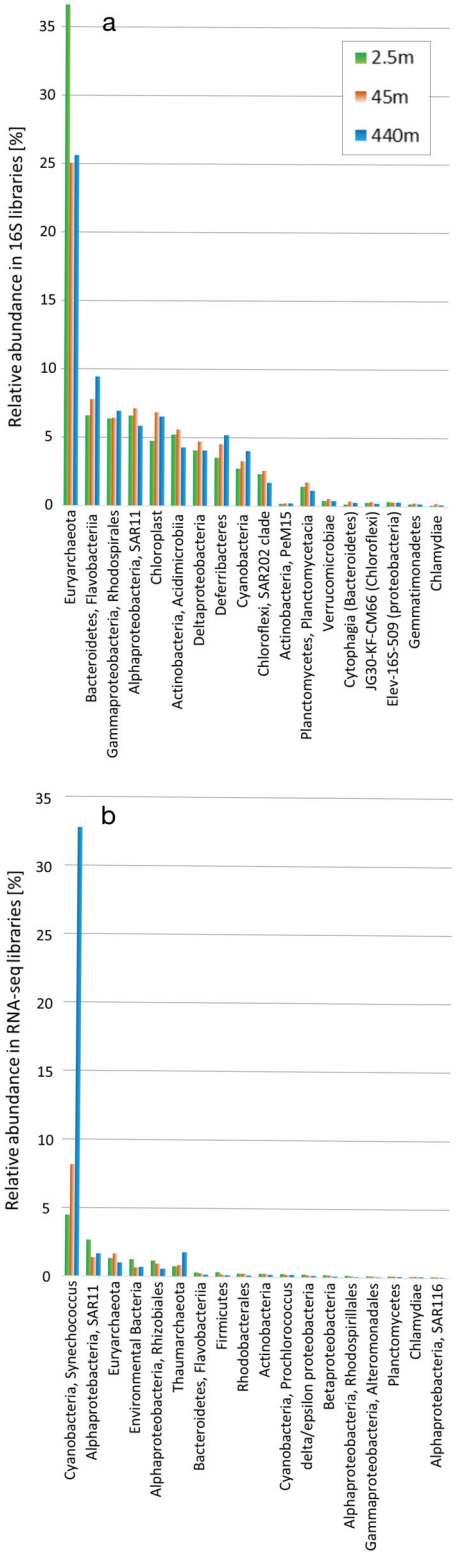

Fig. 2. Relative abundances of the 18 most abundant prokaryotic taxa among (a) 16S rRNA gene amplicon reads and (b) metatranscriptome libraries. Libraries collected from 3 different depths are color labeled. Sequences annotated as 'environmental bacteria' are defined by NCBI as environmental sequences that were classified as bacterial

2.5 and 440 m and at 45 m, suggesting convective control of their vertical distribution (Fig. 2a, Table S1 in Supplement 2 at www.int-res.com/articles/suppl/a080p223_supp2.xlsx; all supplementary tables are available in Supplement 2). The comparable distribution of photosynthetic cyanobacteria in the photic and aphotic layers (Fig. 1) further supports this conclusion. The 45 m sample was obtained on the same day in the framework of a study that compared different RNA library preparation methods (Hou et al. 2016). However, since this sample was collected several hours after the 2.5 and 440 m samples, we excluded it from the differential expression analysis performed here (detailed below). Although taxonomically similar, observed variations in population composition suggested that, in addition to convection, parameters such as light, nutrients, and biotic interactions regulated population structure. During a deep convection event (0–1500 m) in the NW Mediterranean Sea, relatively similar microbial assemblages were obtained throughout the mixed water column, with the observed compositional variations attributed to gradients of nutrients and organic matter (Severin et al. 2016). In a large-scale metagenomic survey across the Red Sea, altered temperature and nitrate concentrations accounted for >70% of variation in functional and taxonomic characteristics of the microbial populations (Thompson et al. 2017). Temperature was stable throughout the mixed layer, consistent with the rather modest variations in population composition observed here at different depths (Fig. 2a, Table S1). Our limited sample size precluded detailed comparisons of environmental drivers impacting functional and taxonomic traits between depths (e.g. Thompson et al. 2017).

The velocity of convective mixing currents in the Gulf of Aqaba is currently unknown, but models predict that during winter, mixing currents may reach 1 cm s^{-1} (H. Gildor & H. Berman pers. comm.). In the NW Mediterranean where deep mixing occurs (Gulf of Lions), convective mixing velocities ranged from 0.3–10.2 cm s^{-1} (Schott & Leaman 1991). Assuming the current velocity to be ~0.3–1 cm s^{-1}, it will take 14–46 h for a picoplanktonic cell to travel a distance of 500 m (mixed layer depth at the time of sampling). Estimations of *Prochlorococcus* doubling rates in the field range from 0.2–1.4 doublings d^{-1} (Partensky et al. 1999). Growth rates from bacterioplankton batch cultures range from 0.07 d^{-1} for SAR11, 1.05 d^{-1} in *Gammaproteobacteria* (Ferrera et al. 2011), and rates of 0.23–0.47 d^{-1} in cultures of marine archaea (Herndl et al. 2005). In the water column, exposure to various stressors including UV and photo-stress, light deprivation, and high hydrostatic pressure will further alter net growth rates. Taking our conservative estimate of the duration of a complete convection cycle into account, combined with the published range of growth rates, we can assume that division and mortality could have altered the relative abundance of some microbial groups.

The most abundant OTU at all depths was identified as marine group II (MG-II) *Euryarchaeota*, comprising 36% of the 16S community at 2.5 m and ~25% at 440 and 45 m. Our results are consistent with estimates (based on CARD-FISH) of *Euryarchaeota* and *Thaumarchaeota* comprising 20–40% of the prokaryotic community in the Gulf of Aqaba during summer (Ionescu et al. 2009) and suggest that these prokaryotes are abundant throughout the year. Following *Euryarchaeota*, the most abundant groups were *Flavobacteriia* (6.6, 7.8, and 9.4% at 2.5 , 45, and 440 m, respectively), and SAR11 (6.6, 7.1 and 5.8%, respectively; Fig. 2a, Table S1).

Higher relative abundance of certain taxa (SAR11, MG-II *Euryarchaeota*) detected at the photic compared with the aphotic depth (Fig. 2a) corresponds with their ability to use light as an additional energy source (Béjà et al. 2000, Giovannoni et al. 2005a, DeLong & Béjà 2010, Iverson et al. 2012). Vertical mixing also enhances availability of phytoplankton-derived particulate and dissolved organic matter (Heimbürger et al. 2013, Gogou et al. 2014, Severin et al. 2014). This organic matter supports the development of bacteria regularly inhabiting the euphotic zone, such as *Oceanospirillales* and *Flavobacteriales* (Severin et al. 2016). Furthermore, high-density organic particles provide 'hotspots' supporting microbial populations and facilitating recycling of high molecular weight dissolved organic matter (Kirchman 2002, Teeling et al. 2012, Buchan et al. 2014). This may explain the higher relative abundance of *Flavobacteriia* at 440 m depth (Fig. 2a, Table S1).

While direct comparison between 16S amplicon based population composition and RNA-seq based taxonomy of transcriptional activity is problematic (see below), we analyzed the relative share of taxonomic groups in the metatranscriptome by running a similarity search of reads against the NCBI nt database (Fig. 2b). This approach provided a valid estimation of the transcriptional activity of specific taxonomic groups which differed substantially from the 16S-based taxonomic profile (Fig. 2a). Most prominently, the most abundant group in the 16S libraries, *Euryarchaeota*, was ranked third, second, and fourth at 2.5, 45, and 440 m (with 1.3, 1.6, and 1.0%, respectively). Similarly, while 16S analyses ranked *Flavo-*

bacteriia as the second most abundant at all depths with 6.6, 7.8, and 9.4% at 2.5, 45, and 440 m, their transcriptional activity was low, contributing only 0.3% to all RNA reads at 2.5 m, 0.2% at 45 m, and only 0.1% at 440 m. A similar trend was observed for *Rhodospirillales*, which comprised 6.6, 6.4, and 6.9% of the 16S community at these respective depths, and displayed marginal transcriptional activity at all depths (0.04–0.12%). Conversely, *Synechococcus,* with low 16S relative abundance (1.3 and 2.6% of the 16S community at 2.5 and 440 m, respectively), displayed the highest transcriptional activity, contributing 4.5% of all RNA reads at 2.5 m, 8.1% at 45 m, and 32.8% at 440 m. Notably, while *Thaumarchaeota* were not among the 18 most abundant groups in the 16S libraries, they were ranked sixth, fifth, and second in the RNA-seq libraries from 2.5, 45 and 440 m, respectively (relative abundance: 0.7, 0.8, and 1.8%). Ammonia oxidation in *Thaumarchaeota* is light sensitive (Merbt et al. 2012), consistent with their increasing transcriptional activity at the aphotic depth (Fig. 2b).

For eukaryotes, the above analysis is not suitable for a direct comparison between mRNA and 16S rRNA taxonomic distribution, as such a comparison can underestimate abundance. Eukaryotic organisms only contain 16S rRNA genes in their organelles (chloroplasts and mitochondria), of which the number varies within cells in many eukaryotic groups. Thus, although comprising 8.9–18.5% of reads in all RNA-seq libraries (see section 'Taxonomic affiliation of mRNA sequence reads' in Supplement 1), eukaryotes were excluded from this analysis.

Differences between the SILVA database and the nt database, and between organisms, further complicate the comparison between 16S-based population composition and the taxonomic affiliation of metatranscriptome reads. Although the vast majority of 16S reads map to the SILVA database at any taxonomic level (only 0.06–0.1% remained unassigned in our libraries), the assignment of metatranscriptome reads (RNA) to taxa using the nt database was more ambiguous (28.9–49.3% unmapped in our libraries; Table 1). Thus, cultivated and well-studied organisms such as *Synechococcus* are over represented in the nt database with multiple reference genomes, compared to insufficient coverage of groups with few or no reference genomes.

Nevertheless, although the accuracy of representation of the various taxa is limited, our results highlight differences in transcriptional activity between the examined groups. The high transcriptional activity (~4.5 to ~32.8% compared to ~1.3 to ~2.5% of all 16S sequences) observed in *Synechococcus* was not reflected in the groups *Euryarchaeota*, *Flavobacteriia*, SAR202, and others (Fig. 2b). Similar discrepancies between 16S-based population community and taxonomic distribution of RNA reads were found also in Gulf of Mexico microbial communities (Rinta-Kanto et al. 2012). Importantly, the uncoupling of transcript abundance and population composition contributes to the observed differences, with transcript abundance varying on scales of minutes to hours (e.g. Ottesen et al. 2014) compared to the more stable dynamics of population composition. Thus, the time of sampling could further impact the results.

Expression of genes related to metabolic activities in specific taxa

To gain insight into the ecological roles and interactions within the microbial populations, we assessed detailed gene expression in representatives of diverse ecological groups that dominated the 16S and/or metatranscriptome datasets (see Figs. 3 & 4, Tables S2 & S4–S7). We focused on organisms with different ecological roles in the community, with an attempt to shed light on potential interactions and relationships within the microbial population. To assess gene expression in these groups, we mapped group-specific reads to a selected reference genome that recruited the largest fraction of reads of all tested references (see section 'Selection of reference organisms' in Supplement 1). Of all tested cyanobacterial references, the photoautotrophic *Synechococcus* CC9605 recruited the largest fraction of cyanobacterial reads in our datasets and was thus selected as a representative of the cyanobacteria. The unicel-

Table 1. RNA read counts for each level of analysis in the metatranscriptome quality control (QC) and analysis pipelines. Fw: forward reads, Rev: reverse reads, nt: nucleotide database of NCBI

Depth (m)	Read-orientation	No. of reads after QC	Non-rRNA reads	Reads mapped to nt	% reads not mapped to nt
2.5	Fw	78185262	6322603	–	–
	Rev	77676351	6374390	3232132	49.3
45	Fw	71493360	6407153	–	–
	Rev	71291764	6461751	3489718	46
440	Fw	81432159	35905178	–	–
	Rev	80859071	35505554	25243891	28.9

lular *Micromonas* RCC299 of the *Mamiellales* group recruited the largest fraction of reads, and was chosen to represent the predominant picoeukaryote biomass (Fig. 1b). The third representative, highly abundant in the 16S dataset, was SAR11 (Fig. 2a), a photoheterotrophic alphaproteobacterium considered to be the most abundant bacterial group in the oceans (Morris et al. 2002). We additionally selected 2 groups of archaea, highly abundant in the 16S and RNA sequence libraries: *Euryarchaeota* and *Thaumarchaeota*.

Cyanobacteria

Upon assignment of cyanobacterial reads to the *Synechococcus* CC9605 reference genome, we identified 2595 transcripts using our customized TSS prediction pipeline (see section 'TSS prediction' in Supplement 1). These represented 2055 annotated genes in the selected reference genome. The remaining 540 transcripts are versions of genes with multiple transcription start sites, but since no functional differences between these versions are known, only a single gene sequence was used for KEGG analysis. Of the detected genes, 1057 (51%) were assigned to KOs (Table 2). We investigated cyanobacterial metabolism by generating a metabolic network based on these KOs (Fig. S3). The analysis demonstrated that genes transcribed by cyanobacteria were predominantly involved in nucleotide and amino-acid metabolism, carbon fixation, carotenoid and folate biosynthesis, and energy metabolism (TCA cycle, glycolysis, ATP synthesis; Fig. S3). To evaluate the expression of genes not considered in the KEGG database, we ranked the list of cyanobacterial transcripts according to the averaged normalized expression values (Table S2). This approach allowed us to complement the list of functions detected by mapping transcripts to the KEGG database and include the activation of energy metabolism, protein synthesis, and RNA metabolism, by identifying high, but non-differential expression of the *petF-3* gene encoding ferredoxin, as well as genes involved in photosynthesis (*psbE, psbD-2*), ribosomal proteins (*rpmJ*, *rpmI*, *rpsU*), and an RNA-recognition motif containing protein (Syncc9605_1510) (Table S2).

We further characterized depth-specific cyanobacterial metabolism by visualizing the number of overexpressed and functionally (KEGG) defined transcripts from each depth (Fig. 3a). Accordingly, we generated a characteristic profile of metabolic functions per depth. In this visualization, the number of overexpressed genes at a certain depth, that were assigned to the presented pathways, is displayed as the intensity of coloration in the heatmap. Thus, when an equal number of (different) genes assigned to a certain pathway were determined as overexpressed in each of the depths, the pathway as a whole was not considered different between the 2 depths. For the 2.5 m sample, we used the 79 (68%) of the 87 transcribed genes that matched KOs and that were overexpressed compared to 440 m. Upregulated pathways at the surface were related to photosynthesis, chlorophyll biosynthesis, and energy metabolism (Fig. 3a). Glycine dehydrogenase, catalyzing the conversion of glycine to glyoxylate and ammonia and participating in photorespiration, was also overexpressed at 2.5 m (Fig. 3a, Table S2). At 2.5 m depth, high irradiance and super-saturated oxygen concentrations may activate photorespiratory pathways, as observed for *Nodularia*, a cyanobacterium forming summer surface blooms in the Baltic (Kopf et al. 2015). Other transcripts enriched in the 2.5 m sample were related to glutathione metabolism, terpenoid and peptidoglycan biosynthesis, aminoacyl-tRNA biosynthesis, protein export (signal recognition particle), and to isocitrate dehydrogenase (an enzyme involved in carbon metabolism) (Fig. 3a, Table S2).

Table 2. Data underlying the analysis of each taxon examined in detail in the framework of this study. The number of reads assigned to each taxonomic group at each depth, the number of transcripts detected, the number of genes these transcripts correspond to, and the number of KEGG orthologs (KOs) these genes matched are detailed

Taxon	Selected reference	No. of reads at 440 m	No. of reads at 2.5 m	No. of transcripts	No. of genes	No. of KOs
Cyanobacteria	*Synechococcus* CC9605	16403744	603887	2595	2055	1057
Mamiellales	*Micromonas* sp. RCC299	2526910	702446	1689	1289	689
SAR11 clade	*Pelagibacter* sp. HTCC7211	610309	188942	1150	934	717
Euryarchaeota	Customized reference	245399	63897	805	724	447
Thaumarchaeota	Customized reference	526638	30613	736	552	296

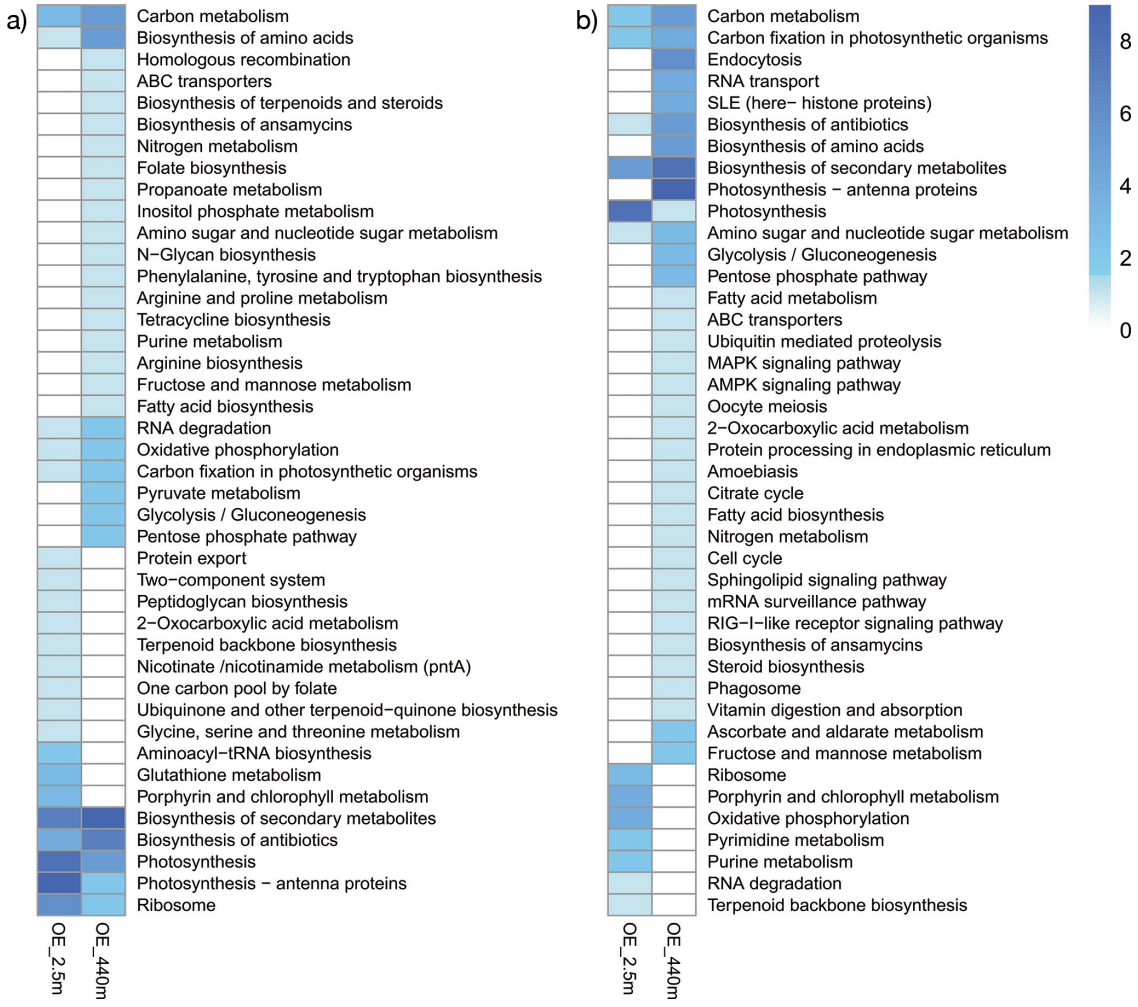

Fig. 3. KEGG pathways characterizing different depths in (a) cyanobacteria and (b) *Mamiellales*. Pathway expression at 2.5 m is presented in the left column while 440 m pathways are presented in the right column. Color scale represents the number of differentially expressed transcripts assigned to each pathway: stronger coloration of a field in the heatmap means a higher number of transcripts overexpressed in the respective depth relative to the other depth (column), that were mapped to the respective pathway (line). OE: overexpression

Compared with the surface (2.5 m) sample, overexpressed KOs from the aphotic (440 m) depth were assigned predominantly to carbon metabolism, pentose phosphate pathway, glycolysis/gluconeogenesis, pyruvate, and biosynthesis of secondary metabolites, antibiotics, and fatty and amino acids (Fig. 3a). Of 104 transcripts overexpressed at 440 m, 42% matched KOs compared with 68% of those overexpressed at the surface. This is probably due to the limited published data existing on aphotic cyanobacterial gene expression. The pentose phosphate pathway produces reductants linking it to anabolic reactions such as fatty acid synthesis (Heise & Fuhrmann 1994) and nitrogen assimilation (Bowsher et al. 1989), and is coupled with carbon recycling in non-photosynthetic plastids (Hartwell et al. 1996). Overall, the overexpression of genes assigned to these pathways at 440 m depth indicates that at the time of sampling, cyanobacteria actively employed many genes involved in the production of secondary metabolites and cell structures within the aphotic depth.

We hence searched for the metabolic basis of this cyanobacterial aphotic activity. *Synechococcus* and other cyanobacteria can grow mixotrophically, using sugars, amino acids, and peptides, both in the laboratory and in their natural habitats (Moore 2013, Swan et al. 2013, Coe et al. 2016, Yelton et al. 2016). We did not detect differentially expressed genes encoding transporters for organic compounds among cyanobacteria in our samples, and expression of these genes was generally low (Table S3).

However, our reference *Synechococcus* CC9605 was isolated from an oligotrophic region in the California Current (Dufresne et al. 2008). In oligotrophic environments, cyanobacteria express reduced numbers of genes encoding organic matter transporters (Yelton et al. 2016). We therefore mapped all cyanobacterial reads from both depths and the 45 m sample mentioned above (Hou et al. 2016) against a customized database containing 26 gene sequences encoding transporters for organic compounds (see section 'Alignment of cyanobacterial reads to carbon transporters' in Supplement 1). The sequences were obtained from 2 *Synechococcus* genomes but included 17 'multispecies' sequences, i.e. sequences that are highly conserved among members of this clade. Of all cyanobacterial sequences, 0.004, 0.002, and 0.003% were mapped to this database at 2.5, 45, and 440 m, respectively. Thus, we detected only a marginal expression of transporters for organic compounds by cyanobacteria in our samples.

Cyanobacteria can also survive deprivation of light by metabolizing intracellular reserves of glycogen (Allen 1984). However, the genes encoding glycogen-degrading enzymes (glycogen/starch/alpha-glucan phosphorylase and glycogen debranching enzymes) exhibited low expression at both depths at the time of sampling. In contrast, we detected highly expressed glycogen synthesis genes *glgB* and *glgC* (Tables S2 & S3). The overexpression of genes involved in the pentose phosphate pathway at 440 m, combined with scarce evidence for the expression of mixotrophy and/or glycogen-degradation related genes (summarized in Table S3), suggest that cyanobacteria in the mixed water column maintained active metabolism at the aphotic depth from carbohydrates synthesized via photosynthesis when the cells were exposed to the light.

Gene expression at 440 m was further characterized by the overexpression of Yfr103, a non-coding RNA of unknown function, yet highly abundant in both natural populations and in cultures of *Synechococcus* and *Prochlorococcus* (Voigt et al. 2014, Hou et al. 2016, Pfreundt et al. 2016a). Transcripts matching all 7 paralogs of *yfr103* in *Synechococcus* CC9605 were at least an order of magnitude more abundant than all other transcripts. Moreover, overexpression at 440 m compared to 2.5 m (Table S2) suggests that Yfr103 may have an important role in the survival of cyanobacterial cells in the aphotic zone.

Prasinophytes – *Mamiellales*

At the time of sampling, picoeukaryotic microalgae dominated the phytoplankton biomass in the water column (Fig. 1) and contributed substantially to the total mRNA pool (Table 2). Of all eukaryotic reads, 74.4% were assigned to *Mamiellales*, with *Micromonas* and *Ostreococcus* recruiting ~95% of the sequences assigned to it. The *Micromonas* sp. RCC299 genome was used as reference for the detailed analysis of gene expression within this group (see Supplements 1 & 2). We detected 1689 *Mamiellales* transcripts that represented 1289 genes annotated in the selected reference genome, of which 689 (53%) were assigned to KOs (Table 2) and constructed a metabolic map (Fig. S4). Highly expressed genes were those involved in photosynthesis and carbon fixation, fatty acid biosynthesis, oxidative phosphorylation, and chlorophyll biosynthesis (Fig. S4). Analysis of all detected *Mamiellales* transcripts (including those that did not match a KO) further revealed a substantial, non-differential expression of ATPase and D1 protein-encoding genes (Table S4).

We generated a depth-specific functional profile based on the number of overexpressed transcripts assigned to each pathway at both depths (Fig. 3b). Out of 79 and 104 overexpressed transcripts at 2.5 and 440 m, 54 (68%) and 44 (42%) matched a KO at the respective depth and were used for further analysis. This analysis revealed that while gene expression at 2.5 m shifted towards energy metabolism and synthesis of some cellular components, highly expressed genes at 440 m were mostly involved in anabolic pathways and phagotrophy, and in transport of organic compatible solutes (see below).

Genes overexpressed at 2.5 m mapped mainly to functions related to energy metabolism, chlorophyll and protein biosynthesis, nucleotide metabolism, terpenoid backbone synthesis, and ribosome, porphyrin, and chlorophyll metabolism (Fig. 3b). Specific transcripts overexpressed at this depth encoded the D2 reaction center and several other photosystem II proteins, 2 F-type ATPase subunits, rRNA genes, and the large subunit of the carbon fixation enzyme ribulose bisphoshate carboxylase oxygenase (RuBisCO) (Table S4). All rRNA genes that were differentially expressed were overexpressed at 2.5 m, corresponding to the overrepresentation of KOs related to ribosomes, and pointing to higher translational activity at the surface (Fig. 3b, Table S4).

In contrast, the overexpressed *Mamiellales* transcripts from 440 m depth were related to endocytosis/phagosome, RNA transport, pentose phosphate

pathway, biosynthesis of various metabolites and cell structures, glycolysis/gluconeogenesis, RNA surveillance, ABC transporters, and vitamin digestion and absorption (Fig. 3b). These results suggest that, similar to cyanobacteria, *Mamiellales* are metabolically active at the aphotic depth with a large fraction of genes assigned to anabolic processes. The upregulation of phagocytosis at 440 m suggests mixotrophy, which is a strategy applied by *Micromonas* under light or nutrient limitation (McKie-Krisberg & Sanders 2014). Yet, comparable to the results obtained for cyanobacteria at this depth, we detected mostly low expression of organic-compound transporters in *Mamiellales* (Table S4). Additional genes overexpressed at 440 m encoded flagellar and motility related proteins, betaine/carnitine/choline transporter family proteins, 2 phosphate:Na^+ symporters, cold-shock DNA- and RNA-binding proteins (*csd*, MICPUN_83180), transcription factors, anaphase-promoting complex protein *cdc20*, and histone proteins, indicating active cell division at depth in these photosynthetic organisms (Table S4). The overexpression of transcripts for the P:Na symporter and the flagellar basal body at 440 m depth implies motility (Throdsen 2012) and acquisition of phosphate by picoeukaryotes at depth. Overexpression of ubiquitin and histone proteins at 440 m indicates that proteasome and chromatin remodeling were active at the aphotic depth in *Mamiellales* while overexpression of betaine/carnitine/choline transporter suggests active osmoregulation and/or utilization of organic compounds for growth.

While the gene encoding the D2 (photosynthetic) protein was overexpressed at 2.5 m, the most highly expressed light harvesting complex proteins were curiously overexpressed at 440 m (Table S4). The photosynthetic enzyme's RuBisCo small and large subunits (SSU, *rbcS* gene and LSU, *rbcL*) were overexpressed at 440 and 2.5 m, respectively. RuBisCo operates as a hexadecamer, made of 8 SSU and 8 LSU protein subunits that are expected to appear in equimolar ratios (reviewed by Hauser et al. 2015). Transcription, translation, and assembly of RuBisCo subunits are subjected to tight regulation (Gutteridge & Gatenby 1995, Yosef et al. 2004). In eukaryotic algae, the genes are split between the chloroplast (*rbcL*) and nuclear genome (*rbcS*), and transcription may proceed independently of protein synthesis. In *Prochlorococcus*, transcript and protein levels were uncoupled for the large RuBisCo subunit (Waldbauer et al. 2012). It is intriguing, yet unclear, why some of these central photosynthetic genes were overexpressed in the dark at 440 m, and further investigation is warranted.

SAR11

We detected 1150 SAR11 transcripts that represented 934 genes from the selected reference genome. Of these, we assigned 717 (77%) to KOs (Table 2), providing the base for a metabolic map (Fig. S5). Genes related to fatty and amino acid biosynthesis, RNA polymerase, oxidative phosphorylation, TCA cycle, and glyoxylate and carbon metabolism were highly expressed (Fig. S5). Of the 75 and 80 genes overexpressed at 2.5 and 440 m, respectively, 95 and 84% were assigned to a KO (Fig. 4a). At 2.5 m depth, pathways related to energy metabolism, protein export, RNA metabolism, and degradation were enriched (Fig. 4a). At 440 m depth, upregulated pathways included amino acid and lipopolysaccharide biosynthesis, the pentose phosphate pathway, fatty acid metabolism, and synthesis of glutathione, starch, and sucrose (Fig. 4a). The term 'amino acid metabolism' was the second and sixth most abundant KEGG term among overexpressed transcripts at 440 and 2.5 m, respectively, with 14 overexpressed KOs at 440 and 7 at 2.5 m. At least 9 of the 14 KOs assigned to amino acid metabolism and overexpressed at 440 m appear to encode enzymes promoting growth and synthesis of metabolites (such as putrescine and glutathione) in contrast with only 4 of the 7 KOs overexpressed at 2.5 m. This suggests that SAR11 metabolism is shifted toward amino acid degradation in the aphotic zone while it can take up and assimilate amino acids in the light (Malmstrom et al. 2004, 2005).

The availability of dissolved inorganic nitrogen and phosphorus can be critically limiting in oligotrophic environments, for both photoautotrophs and bacterioplankton (Moore et al. 2013). After temperature, nitrate was the main driver explaining the functional variations in 45 Red Sea metagenomic samples from both photic and aphotic depths (Thompson et al. 2017). While SAR11 can utilize different nitrogen and phosphorus forms (Thingstad et al. 1998, Malmstrom et al. 2005), the high expression of 2 different ammonium transporters (Table S5) indicated that SAR11 utilized ammonium at the time of sampling. It is likely that competition for this inorganic nitrogen source occurs with cyanobacteria and *Thaumarchaeota*, which also displayed high expression of ammonium transporters (Tables S2 & S7).

In the Red Sea, the expression of nutrient transporters was negatively correlated with the ambient concentration of their respective substrates (Thompson et al. 2017). Availability of N and P and their limitation to microbial populations from the upper

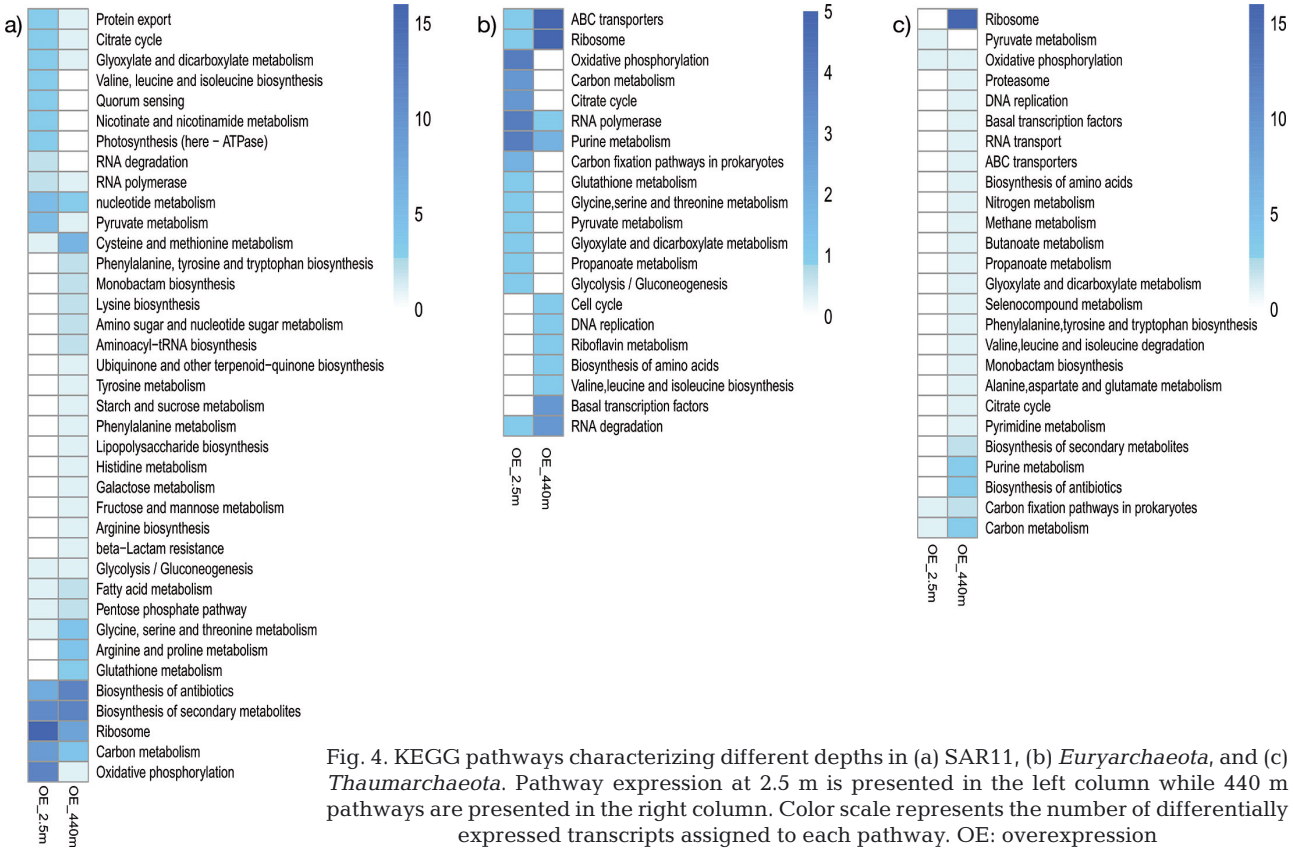

Fig. 4. KEGG pathways characterizing different depths in (a) SAR11, (b) *Euryarchaeota*, and (c) *Thaumarchaeota*. Pathway expression at 2.5 m is presented in the left column while 440 m pathways are presented in the right column. Color scale represents the number of differentially expressed transcripts assigned to each pathway. OE: overexpression

surface layer of the Red Sea varies spatially and temporally (Lindell et al. 2005, Post 2005, Mackey et al. 2007, Thompson et al. 2013, 2017). SAR11 phosphonate and phosphate acquisition genes from a 50 m deep sample (mixed layer depth = 45 m) were underrepresented when compared with other P-limited oligotrophic environments such as the Mediterranean Sea and the North Pacific Subtropical Gyre (Thompson et al. 2013). We observed substantial (yet non-differential) expression of a phosphate ABC transporter (the PB7211_RS05420 gene), and overexpression of the PhoH phosphate starvation protein (Kim et al. 1993) at 440 m. Accordingly, we postulate that SAR11 can experience P starvation at the aphotic depth, and that it assimilates phosphate as a source of P.

Pelagibacter sp. HTCC7211 switches to phosphonate consumption when starved of phosphate (Carini et al. 2014). We did not observe expression of genes related to phosphonate transport and utilization in SAR11, suggesting they were competing with *Euryarchaeota* over inorganic phosphate (see below). Phosphate uptake in heterotrophic populations, including SAR11, may enhance energy production in low-carbon environments as suggested by overexpression of HppA pyrophosphatase in an experimental manipulation of a SAR11-dominated natural bacterioplankton community (Rinta-Kanto et al. 2012). Our metatranscriptomes from both the photic and the aphotic depths displayed high expression of *hppA* in SAR11 (Table S5).

Organic compound transporters (subunits of the spermidine/putrescine and branched amino acid ABC transporters) were among the 20 most highly expressed genes in SAR11 (averaged values between 2.5 and 440 m) yet were not differentially expressed between depths (Table S5). The respective transporter proteins encoded by these genes were also identified in a SAR11 metaproteome generated from a low-nutrient environment in the Sargasso Sea (Sowell et al. 2009). These different transporters contribute to a rather broad nutrient spectrum in an organism with such a small genome (Giovannoni et al. 2005b), enabling its ubiquitous distribution and evolutionary success in the oligotrophic ocean (Morris et al. 2002).

Transcripts related to energy and protein folding (*dnaK*) characterized surface gene expression in SAR11, while expression of anabolic transcripts (genes involved in the synthesis of cellular envelope

and lipopolysaccharides, amino acids, and nucleotides) predominated in the SAR11 population from the aphotic 440 m depth (Fig. 4a, Table S5). Similar to photoautotrophs, energy-starved SAR11 utilizes light for energy production (Steindler et al. 2011). Our observations, showing highly expressed genes for energy metabolism in the photic zone and anabolic-related genes highly expressed aphotically, suggest that light availability modulates transcription during winter mixing. Activation of deoxyribodipyrimidine photolyase, which mitigates DNA UV damage by repairing UV-induced thymidine dimers, shows an acclimation response to high surface irradiance similar to that observed for surface microbial communities from the North Pacific Subtropical Gyre (DeLong et al. 2006). The high expression of this gene at 2.5 m is consistent with the high PAR measured during sampling (1278 µmol photons m^{-2} s^{-1} at the surface; Pfreundt et al. 2014). In addition to high irradiance and UV damage, other stressors may also impact SAR11 activity as we observed high, non-differential, expression of the GroES chaperone (Hightower 1991, Frydman 2001) and the AAA+ FtsH proteases that are essential for proteolysis of regulatory proteins under environmental stress (Deuerling et al. 1995, Herman et al. 1995, Melchers et al. 1998). In bacteria, *ftsH* is involved in heat shock responses and in proteolysis of phage proteins (Langklotz et al. 2012) (Table S5).

Archaea

Uncultivated MG-II *Euryarchaeota* constituted the largest fraction of the microbial community, comprising 25–36% of the 16S community at the time of sampling (Fig. 2a). Although much less abundant, the mRNA read abundance of *Thaumarchaeota* was comparable to that of *Euryarchaeota* (Fig. 2b). Representatives of these archaeal phyla are readily found in high abundances in several marine (and terrestrial) ecosystems (reviewed by Schleper et al. 2005). The metabolic lifestyle of these 2 archaeal phyla is not fully understood and probably includes different trophic lifestyles.

Thaumarchaeota include chemoautotrophic representatives that acquire energy via ammonia oxidation (Könneke et al. 2005), as supported by the wide distribution of thaumarchaeal ammonia oxidase genes in coastal (Monterey Bay) and pelagic (North Pacific Subtropical Gyre) environments (Mincer et al. 2007). Both *Thaumarchaeota* and *Euryarchaeota* can also consume amino acids, suggesting a hetero- or mixotrophic lifestyle in several of their representative species (Ouverney & Fuhrman 2000, Herndl et al. 2005). *Thaumarchaeota* can use bicarbonate as a carbon resource, suggesting autotrophy (Ingalls et al. 2006). Yet, bicarbonate uptake rates are low compared to other prokaryotes (Herndl et al. 2005, Alonso-Sáez et al. 2012, Callieri et al. 2014). Urea uptake by *Thaumarchaeota* led to the hypothesis that urea represents an important resource for both inorganic carbon and nitrogen in some marine systems and suggested a solution for this apparent paradox (Alonso-Sáez et al. 2012).

Transcription profiles of the 2 archaeal phyla indicated differential utilization of nitrogen resources. In *Euryarchaeota*, genes related to the transport and utilization of amino acids and other nitrogen-containing organic compounds were highly expressed (Table S6). In contrast, these transcripts were not detected in *Thaumarchaeota*, and genes encoding ammonia and urea transporters were ranked fifth and ninth most highly expressed in this phylum, respectively (Table S7). While urea concentrations were not measured, high expression of the urea amidohydrolase gene (Table S7) in *Thaumarchaeota* suggests urea metabolism, perhaps as both a carbon and nitrogen resource (Alonso-Sáez et al. 2012). Additionally, high *amt* ammonia permease expression (Table S7) indicates that *Thaumarchaeota* also use ammonia as a nitrogen resource. In addition to its role as an electron donor for catabolism, expression of glutamine synthetase (Table S7) suggested ammonia was assimilated into glutamine.

Thaumarchaeota and *Euryarchaeota* also appear to utilize different phosphorus sources. In *Thaumarchaeota*, a *phnD* phosphonate transporter transcript was enriched and overexpressed at 440 m depth compared to 2.5 m (Table S7). In *Euryarchaeota*, we detected substantial expression of inorganic phosphate transporters, including a putative low affinity inorganic phosphate transporter and the PstS phosphate binding protein of an ABC transporter (Table S6).

The gene expression metabolic map of *Euryarchaeota* (Fig. S6) was based on 805 identified euryarchaeal transcripts which matched 724 genes in the reference pan-genome, 447 (62%) of which corresponded to a KO (Table 2). Transcripts related to the biosynthesis of riboflavin (vitamin B2) and ubiquinone (a central compound of the aerobic respiratory electron transport chain) predominated. A list of all identified euryarchaeal transcripts, including those that were not assigned to the KEGG database (Table S6), revealed that 7 out of the top 20 ex-

pressed euryarchaeal transcripts showed no differential expression between the different depths (Table S6). These transcripts included *boxB* (benzoyl-CoA oxygenase subunit beta), *fdxA* (iron sulfur containing ferredoxin), *ubiB*, *pdxS/pdx1* (vitamin B6 synthesis), and *ribA* (riboflavin biosynthesis), implying utilization of benzoate as an organic carbon source (Zaar et al. 2004), and biosynthesis of vitamins B2 and B6.

Euryarchaea also revealed depth-specific expression, with 21 overexpressed genes with KO attribution at 2.5 m (78% of all overexpressed KOs at this depth). Upregulation was indicated in pathways related to glycolysis, oxidative phosphorylation, the TCA cycle, amino acid, glutathione and carbon metabolism (Fig. 4b). More specifically, KOs overexpressed at 2.5 m included: a broad specificity leucyl-aminopeptidase involved in protein housekeeping (eury_gene69), *pdhD* pyruvate dehydrogenase gene (TCA cycle), *ntpA* and *ntpB* encoding V/A type ATPase (oxidative phosphorylation), and *sdhB*/*frdB*—the Fe-S subunit of succinate dehydrogenase/fumarate reductase (TCA cycle, oxidative phosphorylation). Transcripts overexpressed at 2.5 m, but without KEGG assignment (Table S6), included the *dnaK* chaperone and the *phrB* photolyase involved in the UV stress response. Additional genes overexpressed at 2.5 m were involved in transcription (*rpoA*, *gyrB*), iron sulfur cluster assembly (*sufD,* also overexpressed in SAR11 at 2.5 m), 3 F-type ATP synthase subunits, and a branched amino acid ABC transporter subunit (Table S6). Thus, surface enriched euryarchaeal transcripts indicated active energy metabolism, phosphate and amino acid transport, and stress responses.

In contrast, the 32 KOs overexpressed at 440 m (68% of all overexpressed euryarchaeal KOs at this depth) included genes assigned to pathways related to DNA replication and cell cycle, riboflavin metabolism (*rfk*), amino acid biosynthesis (*ilvD*), transcription initiation (*tbp*), and RNA polymerase (*rpoA*) (Fig. 4b, Table S6). Other overexpressed genes included *livK* (a component of the leucine transport system), *pbuG* (xanthine/uracil transport), and *ftsZ* (cell division), pointing to active nucleotide transport and cell division in the aphotic depth (Table S6).

Our results show that *Euryarchaeota* activated energy metabolism related genes at the photic depth while upregulating cell cycle genes, as well as genes involved in amino acid biosynthesis and transcription in the aphotic zone at 440 m depth (Fig. 4b, Table S6). Archaea can synthesize riboflavin (Fischer et al. 2004), and genes involved in pyridoxine biosynthesis were found in euryarchaeal genomes (Ehrenshaft et al. 1999, Osmani et al. 1999).

A total of 736 thaumarchaeal transcripts were detected, representing 552 genes in the selected thaumarchaeal pan-genome. Of these, 296 (54%) matched a KO (Table 2) from which we constructed a metabolic map (Fig. S7). Here, we observed high expression of *nadA,* involved in the biosynthesis of the central intermediate nicotinamide adenine dinucleotide (NAD), *folE*, and *dxs* (folate biosynthesis and thiamine metabolism), urease, the RNA polymerase omega subunit (*rpb6*), and genes related to nucleotide metabolism (Fig. S7, Table S7). Our observations suggest that *Euryarchaeota* and *Thaumarchaeota* may be a source of vitamins B1 (thiamin), B2, B6, and B9 (folate) in the water column, analogous to observations on the provision of vitamins such as thiamin (B1) (Paerl et al. 2017) and cobalamin (B12) (Bonnet et al. 2010) by certain members of the community. This is further supported by the discovery of a complete cobalamin biosynthesis pathway in *Thaumarchaeota* (Doxey et al. 2015).

Thaumarchaeal transcripts that were highly expressed at both depths included 2 *amt* ammonia permease genes, an active urea transporter (Thaumarchaeote gene2780, GenBank accession: AIF12188.1), an *arsR* transcription factor (regulating among others the expression of the *phoP* alkaline phosphatase; Gao et al. 2011), and a blue copper domain-containing protein with a C terminal PEFG domain (cupredoxin, involved in unknown redox processes) (Table S7). These results suggest that nutrient uptake and assimilation indicated by genes for ammonia and urea transport, as well as energy metabolism and phosphate stress responses are important features of *Thaumarchaeota* that are independent of depth and light availability in this system.

The depth-specific functional profile (based on the number of transcripts recruited to pathways and overexpressed at each depth) was similar to that derived for *Euryarchaeota*. Upregulated genes were involved in energy and carbon metabolism pathways at the surface, while at 440 m depth anabolic pathways were upregulated (Fig. 4c). At 2.5 m, the 5 overexpressed transcripts with KO attribution (38.5% of the 14 overexpressed KOs at this depth) were assigned to the FtsH protease (cell division, stress response), *rpoH* sigma-32 factor involved in heat shock response in *Escherichia coli* (Fujita & Ishihama 1987), BIRC6/BRUCE (inhibitor of apoptosis and involved in proteolysis; Bartke et al. 2004), ubiquinol–cytochrome C reductase (oxidative phosphorylation), and *ppdK* encoding pyruvate phosphate dikinase

producing phosphoenolpyruvate (PEP), a key compound in carbon metabolism and glycolysis.

Other genes overexpressed at 2.5 m (not matching a KO) included another urea transporter gene (GenBank accession AIF00862.1) and conserved proteins implicated in secretion (Table S7).

At 440 m, 41 out of the 77 upregulated thaumarchaeal transcripts (53%) were assigned to KOs, and were coupled with amino acid and secondary metabolite biosynthesis, DNA replication, transcription initiation, and induction of ribosomal proteins (Fig. 4c). Other upregulated pathways at 440 m included amino acid degradation, nitrogen metabolism (ammonia monooxygenase), nucleotide metabolism (*comEB*–dCMP deaminase), proteasome, and ABC transporters (*phnD* phosphonate transporter subunit). The *amoB* and *amoX* genes were also overexpressed at 440 m (ammonia monooxygenase subunits B and X), in contrast to the *amoC* subunit that was not differentially expressed. Differentially expressed sulfate adenylyltransferase (*met3*), adenylylsulfate kinase (*cysC*), and rhodanese-related sulfur transferase (Table S7) further indicated active sulfate assimilation and metabolism at 440 m.

The archaeal profiles are consistent with the expression patterns obtained for SAR11 and cyanobacteria. The surface sample at 2.5 m was characterized by overexpressed energy metabolism-related genes while the predominant transcripts at 440 m depth were related to replication and synthesis (anabolism). Interpretation of this result is not as intuitive as for photoautotrophic organisms that utilize light to produce energy. Photosynthesis-derived matter (i.e. organic carbon) serves as an energy source for heterotrophic bacterioplankton and would thus be more available for heterotrophic utilization in the photic layer. The data indicate that during deep mixing, heterotrophs will increase energy (carbon) metabolism at the illuminated surface waters where carbon fixation occurs and enhance production of cellular components and secondary metabolites at the aphotic depth.

Conclusions

The present study provides insights into microbial gene expression and community composition in the photic and aphotic depths of a deep-mixed water column in the Gulf of Aqaba, Red Sea. For both photoautotropic and heterotrophic organisms, the RNA obtained at the surface was enriched with transcripts associated with energy metabolism and stress responses, in contrast to high expression of genes associated with biosynthesis of secondary metabolites and cellular components, replication, and growth, which characterized the aphotic depth. Moreover, although picoeukaryotic algae of the *Mamiellales* group appeared to employ phagotrophy and/or mixotrophy at 440 m depth, we did not detect cyanobacterial gene expression linked to mixotrophy or the utilization of glycogen reserves. Combined with the negligible expression of transporters of organic compounds, our data suggest that photosynthates produced in the photic zone support cyanobacterial metabolism under aphotic conditions until the cells encounter light once more. Our data also reveal that archaea, primarily MG-II *Euryarchaeota* and *Thaumarchaeota*, comprised a large fraction of the microbial community at the time of sampling, and that niche partitioning based on differential utilization of nitrogen and phosphorus sources occurs between these 2 archaeal groups.

Acknowledgements. This work was supported by the Assemble (Association of European Marine Biological Laboratories) Infrastructure Access Call 5 to the Interuniversity Institute for Marine Sciences, Eilat, (IUI) Israel, by a BMBF-MOST joint German-Israeli research project, project number GR2378/03F0640A to I.B.-F. and W.R.H., and by the EU project MaCuMBA (Marine Microorganisms: Cultivation Methods for Improving their Biotechnological Applications; grant agreement no: 311975) to W.R.H. The financial support to S.H. by the China Scholarship Council is gratefully acknowledged. This work is in partial fulfillment of a PhD requirement for D.M., who was also supported by a Presidents' Fellowship from Bar Ilan University. We thank the IUI logistic team and captain and crew of the RV 'Sam Rothberg' for help at sea and H. Elifantz for help during manuscript preparation.

LITERATURE CITED

Allen MM (1984) Cyanobacterial cell inclusions. Annu Rev Microbiol 38:1–25

Alonso-Sáez L, Waller AS, Mende DR, Bakker K and others (2012) Role for urea in nitrification by polar marine archaea. Proc Natl Acad Sci USA 109:17989–17994

Bartke T, Pohl C, Pyrowolakis G, Jentsch S (2004) Dual role of BRUCE as an antiapoptotic IAP and a chimeric E2/E3 ubiquitin ligase. Mol Cell 14:801–811

Béjà O, Aravind L, Koonin EV, Suzuki MT and others (2000) Bacterial rhodopsin: evidence for a new type of phototrophy in the sea. Science 289:1902–1906

Bonnet S, Webb EA, Panzeca C, Karl DM, Capone DG, Wilhelmy SAS (2010) Vitamin B12 excretion by cultures of the marine cyanobacteria *Crocosphaera* and *Synechococcus*. Limnol Oceanogr 55:1959–1964

Bowsher CG, Hucklesby DP, Emes MJ (1989) Nitrite reduction and carbohydrate metabolism in plastids purified from roots of *Pisum sativum* L. Planta 177:359–366

Brinkhoff T, Muyzer G (1997) Increased species diversity

and extended habitat range of sulfur-oxidizing *Thiomicrospira* spp. Appl Environ Microbiol 63:3789–3796

Buchan A, LeCleir GR, Gulvik CA, González JM (2014) Master recyclers: features and functions of bacteria associated with phytoplankton blooms. Nat Rev Microbiol 12: 686–698

Buitenhuis ET, Li WKW, Vaulot D, Lomas MW and others (2012) Picophytoplankton biomass distribution in the global ocean. Earth Syst Sci Data 4:37–46

Callieri C, Coci M, Eckert EM, Salcher MM, Bertoni R (2014) Archaea and Bacteria in deep lake hypolimnion: in situ dark inorganic carbon uptake. J Limnol 73:47–54

Carini P, White AE, Campbell EO, Giovannoni SJ (2014) Methane production by phosphate-starved SAR11 chemoheterotrophic marine bacteria. Nat Commun 5: 4346

Carlson DF, Fredj E, Gildor H (2014) The annual cycle of vertical mixing and restratification in the Northern Gulf of Eilat/Aqaba (Red Sea) based on high temporal and vertical resolution observations. Deep-Sea Res I 84:1–17

Charuvaka A, Rangwala H (2011) Evaluation of short read metagenomic assembly. BMC Genomics 12(Suppl 2):S8

Coe A, Ghizzoni J, LeGault K, Biller S, Roggensack SE, Chisholm SW (2016) Survival of *Prochlorococcus* in extended darkness. Limnol Oceanogr 61:1375–1388

DeLong EF, Béjà O (2010) The light-driven proton pump proteorhodopsin enhances bacterial survival during tough times. PLOS Biol 8:e1000359

DeLong EF, Preston CM, Mincer T, Rich V and others (2006) Community genomics among stratified microbial assemblages in the ocean's interior. Science 311:496–503

Deschamps P, Zivanovic Y, Moreira D, Rodriguez-Valera F, López-García P (2014) Pangenome evidence for extensive interdomain horizontal transfer affecting lineage core and shell genes in uncultured planktonic Thaumarchaeota and Euryarchaeota. Genome Biol Evol 6: 1549–1563

Deuerling E, Paeslack B, Schumann W (1995) The *ftsH* gene of *Bacillus subtilis* is transiently induced after osmotic and temperature upshift. J Bacteriol 177:4105–4112

Dore JE, Houlihan T, Hebel DV, Tien G, Tupas L, Karl DM (1996) Freezing as a method of sample preservation for the analysis of dissolved inorganic nutrients in seawater. Mar Chem 53:173–185

Doxey AC, Kurtz DA, Lynch MD, Sauder LA, Neufeld JD (2015) Aquatic metagenomes implicate *Thaumarchaeota* in global cobalamin production. ISME J 9:461–471

Dufresne A, Ostrowski M, Scanlan DJ, Garczarek L and others (2008) Unraveling the genomic mosaic of a ubiquitous genus of marine cyanobacteria. Genome Biol 9:R90

Edgar RC (2013) UPARSE: highly accurate OTU sequences from microbial amplicon reads. Nat Methods 10:996–998

Ehrenshaft M, Bilski P, Li MY, Chignell CF, Daub ME (1999) A highly conserved sequence is a novel gene involved in de novo vitamin B6 biosynthesis. Proc Natl Acad Sci USA 96:9374–9378

Ferreira AJS, Siam R, Setubal JC, Moustafa A and others (2014) Core microbial functional activities in ocean environments revealed by global metagenomic profiling analyses. PLOS ONE 9:e97338

Ferrera I, Gasol JM, Sebastián M, Hojerová E, Koblížek M (2011) Comparison of growth rates of aerobic anoxygenic phototrophic bacteria and other bacterioplankton groups in coastal Mediterranean waters. Appl Environ Microbiol 77:7451–7458

Fischer M, Schott AK, Römisch W, Ramsperger A and others (2004) Evolution of vitamin B_2 biosynthesis. A novel class of riboflavin synthase in Archaea. J Mol Biol 343:267–278

Frydman J (2001) Folding of newly translated proteins in vivo: the role of molecular chaperones. Annu Rev Biochem 70:603–647

Fujita N, Ishihama A (1987) Heat-shock induction of RNA polymerase sigma-32 synthesis in *Escherichia coli*: transcriptional control and a multiple promoter system. Mol Gen Genet MGG 210:10–15

Gao CH, Yang M, He ZG (2011) An ArsR-like transcriptional factor recognizes a conserved sequence motif and positively regulates the expression of *phoP* in mycobacteria. Biochem Biophys Res Commun 411:726–731

Genin A, Lazar B, Brenner S (1995) Vertical mixing and coral death in the Red Sea following the eruption of Mount Pinatubo. Nature 377:507–510

Ghiglione JF, Mevel G, Pujo-Pay M, Mousseau L, Lebaron P, Goutx M (2007) Diel and seasonal variations in abundance, activity, and community structure of particle-attached and free-living bacteria in NW Mediterranean Sea. Microb Ecol 54:217–231

Ghiglione JF, Palacios C, Marty JC, Mével G and others (2008) Role of environmental factors for the vertical distribution (0–1000 m) of marine bacterial communities in the NW Mediterranean Sea. Biogeosciences 5:1751–1764

Giovannoni SJ, Bibbs L, Cho JC, Stapels MD and others (2005a) Proteorhodopsin in the ubiquitous marine bacterium SAR11. Nature 438:82–85

Giovannoni SJ, Tripp HJ, Givan S, Podar M and others (2005b) Genome streamlining in a cosmopolitan oceanic bacterium. Science 309:1242–1245

Gogou A, Sanchez-Vidal A, Durrieu de Madron X, Stavrakakis S and others (2014) Carbon flux to the deep in three open sites of the Southern European Seas (SES). J Mar Syst 129:224–233

Gutteridge S, Gatenby AA (1995) Rubisco synthesis, assembly, mechanism, and regulation. Plant Cell 7:809

Hartwell J, Bowsher CG, Emes MJ (1996) Recycling of carbon in the oxidative pentose phosphate pathway in non-photosynthetic plastids. Planta 200:107–112

Hauser T, Popilka L, Hartl FU, Hayer-Hartl M (2015) Role of auxiliary proteins in Rubisco biogenesis and function. Nat Plants 1:15065

Heimbürger LE, Lavigne H, Migon C, D'Ortenzio F, Estournel C, Coppola L, Miquel JC (2013) Temporal variability of vertical export flux at the DYFAMED time-series station (Northwestern Mediterranean Sea). Prog Oceanogr 119:59–67

Heise KP, Fuhrmann J (1994) Factors controlling medium-chain fatty acid synthesis in plastids from *Cuphea* embryos. Prog Lipid Res 33:87–95

Herman C, Thévenet D, D'Ari R, Bouloc P (1995) Degradation of sigma 32, the heat shock regulator in *Escherichia coli*, is governed by HflB. Proc Natl Acad Sci USA 92: 3516–3520

Herndl GJ, Reinthaler T, Teira E, van Aken H, Veth C, Pernthaler A, Pernthaler J (2005) Contribution of archaea to total prokaryotic production in the deep Atlantic Ocean. Appl Environ Microbiol 71:2303–2309

Hightower LE (1991) Heat shock, stress proteins, chaperones, and proteotoxicity. Cell 66:191–197

Hou S, Pfreundt U, Miller D, Berman-Frank I, Hess WR (2016) mdRNA-Seq analysis of marine microbial communities from the northern Red Sea. Sci Rep 6:35470

Ingalls AE, Shah SR, Hansman RL, Aluwihare LI, Santos GM, Druffel ER, Pearson A (2006) Quantifying archaeal community autotrophy in the mesopelagic ocean using natural radiocarbon. Proc Natl Acad Sci USA 103: 6442–6447

Ionescu D, Penno S, Haimovich M, Rihtman B and others (2009) Archaea in the Gulf of Aqaba. FEMS Microbiol Ecol 69:425–438

Iverson V, Morris RM, Frazar CD, Berthiaume CT, Morales RL, Armbrust EV (2012) Untangling genomes from metagenomes: revealing an uncultured class of marine Euryarchaeota. Science 335:587–590

Kanehisa M, Goto S (2000) KEGG: Kyoto Encyclopedia of Genes and Genomes. Nucleic Acids Res 28:27–30

Kanehisa M, Sato Y, Morishima K (2016) BlastKOALA and GhostKOALA: KEGG tools for functional characterization of genome and metagenome sequences. J Mol Biol 428:726–731

Karl DM, Tien G (1992) MAGIC: a sensitive and precise method for measuring dissolved phosphorus in aquatic environments. Limnol Oceanogr 37:105–116

Karl DM, Tien G, Dore J, Winn CD (1993) Total dissolved nitrogen and phosphorus concentrations at US-JGOFS station ALOHA: Redfield reconciliation. Mar Chem 41: 203–208

Kiełbasa SM, Wan R, Sato K, Horton P, Frith MC (2011) Adaptive seeds tame genomic sequence comparison. Genome Res 21:487–493

Kim SK, Makino K, Amemura M, Shinagawa H, Nakata A (1993) Molecular analysis of the *phoH* gene, belonging to the phosphate regulon in *Escherichia coli*. J Bacteriol 175:1316–1324

Kirchman DL (2002) The ecology of *Cytophaga–Flavobacteria* in aquatic environments. FEMS Microbiol Ecol 39: 91–100

Klindworth A, Pruesse E, Schweer T, Peplies J, Quast C, Horn M, Glöckner FO (2013) Evaluation of general 16S ribosomal RNA gene PCR primers for classical and next-generation sequencing-based diversity studies. Nucleic Acids Res 41:e1

Könneke M, Bernhard AE, de la Torre JR, Walker CB, Waterbury JB, Stahl DA (2005) Isolation of an autotrophic ammonia-oxidizing marine archaeon. Nature 437:543–546

Kopf M, Möke F, Bauwe H, Hess WR, Hagemann M (2015) Expression profiling of the bloom-forming cyanobacterium *Nodularia CCY9414* under light and oxidative stress conditions. ISME J 9:2139–2152

Korlević M, Pop Ristova P, Garić R, Amann R, Orlić S (2015) Bacterial diversity in the South Adriatic Sea during a strong, deep winter convection year. Appl Environ Microbiol 81:1715–1726

Kriest I, Oschlies A (2007) Modelling the effect of cell-size-dependent nutrient uptake and exudation on phytoplankton size spectra. Deep-Sea Res I 54:1593–1618

Langklotz S, Baumann U, Narberhaus F (2012) Structure and function of the bacterial AAA protease FtsH. Biochim Biophys Acta 1823:40–48

Lazar B, Erez J, Silverman J, Rivlin T and others (2008) Recent environmental changes in the chemical-biological oceanography of the Gulf of Aqaba (Eilat). In: Por FD (ed) Aqaba-Eilat, the improbable gulf: environment, biodiversity and preservation. Magnes Press, Jerusalem, p 49–62

Li M, Baker BJ, Anantharaman K, Jain S, Breier JA, Dick GJ (2015) Genomic and transcriptomic evidence for scavenging of diverse organic compounds by widespread deep-sea archaea. Nat Commun 6:8933

Lindell D, Post AF (1995) Ultraphytoplankton succession is triggered by deep winter mixing in the Gulf of Aqaba (Eilat), Red Sea. Limnol Oceanogr 40:1130–1141

Lindell D, Penno S, Al-Qutob M, David E, Rivlin T, Lazar B, Post AF (2005) Expression of the nitrogen stress response gene *ntcA* reveals nitrogen sufficient *Synechococcus* populations in the oligotrophic northern Red Sea. Limnol Oceanogr 50:1932

Mackey KR, Labiosa RG, Calhoun M, Street JH, Post AF, Paytan A (2007) Phosphorus availability, phytoplankton community dynamics, and taxon-specific phosphorus status in the Gulf of Aqaba, Red Sea. Limnol Oceanogr 52:873–885

Malmstrom RR, Kiene RP, Cottrell MT, Kirchman DL (2004) Contribution of SAR11 bacteria to dissolved dimethylsulfoniopropionate and amino acid uptake in the North Atlantic Ocean. Appl Environ Microbiol 70:4129–4135

Malmstrom RR, Cottrell MT, Elifantz H, Kirchman DL (2005) Biomass production and assimilation of dissolved organic matter by SAR11 bacteria in the Northwest Atlantic Ocean. Appl Environ Microbiol 71:2979–2986

Marie D, Partensky F, Jacquet S, Vaulot D (1997) Enumeration and cell cycle analysis of natural populations of marine picoplankton by flow cytometry using the nucleic acid stain SYBR Green I. Appl Environ Microbiol 63: 186–193

Massana R, Murray AE, Preston CM, DeLong EF (1997) Vertical distribution and phylogenetic characterization of marine planktonic archaea in the Santa Barbara Channel. Appl Environ Microbiol 63:50–56

McKie-Krisberg ZM, Sanders RW (2014) Phagotrophy by the picoeukaryotic green alga *Micromonas*: implications for Arctic Oceans. ISME J 8:1953–1961

Meeder E, Mackey KRM, Paytan A, Shaked Y and others (2012) Nitrite dynamics in the open ocean — clues from seasonal and diurnal variations. Mar Ecol Prog Ser 453: 11–26

Melchers K, Wiegert T, Buhmann A, Postius S, Schäfer KP, Schumann W (1998) The *Helicobacter felis ftsH* gene encoding an ATP-dependent metalloprotease can replace the *Escherichia coli* homologue for growth and phage λ lysogenization. Arch Microbiol 169:393–396

Mende DR, Waller AS, Sunagawa S, Järvelin AI and others (2012) Assessment of metagenomic assembly using simulated next generation sequencing data. PLOS ONE 7: e31386

Merbt SN, Stahl DA, Casamayor EO, Martí E, Nicol GW, Prosser JI (2012) Differential photoinhibition of bacterial and archaeal ammonia oxidation. FEMS Microbiol Lett 327:41–46

Miller DR, Pfreundt U, Elifantz H, Hess WR, Berman-Frank I (2017) Microbial metatranscriptomes from the thermally stratified Gulf of Aqaba/Eilat during summer. Mar Genomics 32:23–26

Mincer TJ, Church MJ, Taylor LT, Preston C, Karl DM, DeLong EF (2007) Quantitative distribution of presumptive archaeal and bacterial nitrifiers in Monterey Bay and the North Pacific Subtropical Gyre. Environ Microbiol 9: 1162–1175

Moore CM, Mills MM, Arrigo KR, Berman-Frank I and others (2013) Processes and patterns of oceanic nutrient limitation. Nat Geosci 6:701–710

Moore LR (2013) More mixotrophy in the marine microbial mix. Proc Natl Acad Sci USA 110:8323–8324
Morris RM, Rappe MS, Connon S, Virgin KL, Siebold WA, Carlson CA, Giovanonni SJ (2002) SAR11 clade dominates ocean surface bacterioplankton communities. Nature 420:806–810
Olson RJ, Chisholm SW, Zettler ER, Altabet MA, Dusenberry JA (1990) Spatial and temporal distributions of prochlorophyte picoplankton in the North Atlantic Ocean. Deep-Sea Res Part A 37:1033–1051
Osmani AH, May GS, Osmani SA (1999) The extremely conserved *pyroA* gene of *Aspergillus nidulans* is required for pyridoxine synthesis and is required indirectly for resistance to photosensitizers. J Biol Chem 274: 23565–23569
Ottesen EA, Young CR, Gifford SM, Eppley JM and others (2014) Multispecies diel transcriptional oscillations in open ocean heterotrophic bacterial assemblages. Science 345:207–212
Ouverney CC, Fuhrman JA (2000) Marine planktonic archaea take up amino acids. Appl Environ Microbiol 66: 4829–4833
Paerl RW, Bouget FY, Lozano JC, Vergé V and others (2017) Use of plankton-derived vitamin B1 precursors, especially thiazole-related precursor, by key marine picoeukaryotic phytoplankton. ISME J 11:753–765
Partensky F, Hess WR, Vaulot D (1999) *Prochlorococcus*, a marine photosynthetic prokaryote of global significance. Microbiol Mol Biol Rev 63:106–127
Pfreundt U, Miller D, Adusumilli L, Stambler N, Berman-Frank I, Hess WR (2014) Depth dependent metatranscriptomes of the marine pico-/nanoplanktonic communities in the Gulf of Aqaba/Eilat during seasonal deep mixing. Mar Genomics 18:93–95
Pfreundt U, Spungin D, Bonnet S, Berman-Frank I, Hess WR (2016a) Global analysis of gene expression dynamics within the marine microbial community during the VAHINE mesocosm experiment in the southwest Pacific. Biogeosciences 13:4135–4149
Pfreundt U, Van Wambeke F, Caffin M, Bonnet S, Hess WR (2016b) Succession within the prokaryotic communities during the VAHINE mesocosms experiment in the New Caledonia lagoon. Biogeosciences 13:2319–2337
Pinto FL, Thapper A, Sontheim W, Lindblad P (2009) Analysis of current and alternative phenol based RNA extraction methodologies for cyanobacteria. BMC Mol Biol 10: 79–86
Post AF (2005) Nutrient limitation of marine cyanobacteria. In: Huisman J, Matthijs HCP, Visser PM (eds) Harmful cyanobacteria. Springer, Dordrecht, p 87–107
Raven JA, Kübler JE (2002) New light on the scaling of metabolic rate with the size of algae. J Phycol 38:11–16
Reiss Z, Hottinger L (1984) The Gulf of Aqaba, ecological micropaleontology. Springer, Berlin
Rinta-Kanto JM, Sun S, Sharma S, Kiene RP, Moran MA (2012) Bacterial community transcription patterns during a marine phytoplankton bloom. Environ Microbiol 14: 228–239
Robinson MD, Oshlack A (2010) A scaling normalization method for differential expression analysis of RNA-seq data. Genome Biol 11:R25
Schleper C, Jurgens G, Jonuscheit M (2005) Genomic studies of uncultivated archaea. Nat Rev Microbiol 3:479–488
Schott F, Leaman KD (1991) Observations with moored acoustic Doppler current profilers in the convection regime in the Golfe du Lion. J Phys Oceanogr 21:558–574
Severin T, Conan P, Durrieu de Madron X, Houpert L and others (2014) Impact of open-ocean convection on nutrients, phytoplankton biomass and activity. Deep-Sea Res I 94:62–71
Severin T, Sauret C, Boutrif M, Duhaut T and others (2016) Impact of an intense water column mixing (0–1500 m) on prokaryotic diversity and activities during an open-ocean convection event in the NW Mediterranean Sea. Environ Microbiol 18:4378–4390
Sharma CM, Hoffmann S, Darfeuille F, Reignier J and others (2010) The primary transcriptome of the major human pathogen *Helicobacter pylori.* Nature 464:250–255
Sosik HM, Olson RJ, Armbrust EV (2010) Flow cytometry in phytoplankton research. In: Suggett DJ, Prášil O, Borowitzka MA (eds) Chlorophyll *a* fluorescence in aquatic sciences: methods and applications. Springer, Dordrecht, p 171–185
Sowell SM, Wilhelm LJ, Norbeck AD, Lipton MS and others (2009) Transport functions dominate the SAR11 metaproteome at low-nutrient extremes in the Sargasso Sea. ISME J 3:93–105
Steindler L, Schwalbach MS, Smith DP, Chan F, Giovannoni SJ (2011) Energy starved *Candidatus* Pelagibacter ubique substitutes light-mediated ATP production for endogenous carbon respiration. PLOS ONE 6:e19725
Swan BK, Tupper B, Sczyrba A, Lauro FM and others (2013) Prevalent genome streamlining and latitudinal divergence of planktonic bacteria in the surface ocean. Proc Natl Acad Sci USA 110:11463–11468
Tamburini C, Garel M, Al Ali B, Mérigot B, Kriwy P, Charrière B, Budillon G (2009) Distribution and activity of bacteria and archaea in the different water masses of the Tyrrhenian Sea. Deep-Sea Res II 56:700–712
Tarazona S, García-Alcalde F, Dopazo J, Ferrer A, Conesa A (2011) Differential expression in RNA-seq: a matter of depth. Genome Res 21:2213–2223
Tatusova T, Ciufo S, Fedorov B, O'Neill K, Tolstoy I (2014) RefSeq microbial genomes database: new representation and annotation strategy. Nucleic Acids Res 42:D553–D559
Teeling H, Fuchs BM, Becher D, Klockow C and others (2012) Substrate-controlled succession of marine bacterioplankton populations induced by a phytoplankton bloom. Science 336:608–611
Thingstad TF, Zweifel UL, Rassoulzadegan F (1998) P limitation of heterotrophic bacteria and phytoplankton in the northwest Mediterranean. Limnol Oceanogr 43:88–94
Thompson LR, Field C, Romanuk T, Ngugi D, Siam R, El Dorry H, Stingl U (2013) Patterns of ecological specialization among microbial populations in the Red Sea and diverse oligotrophic marine environments. Ecol Evol 3: 1780–1797
Thompson LR, Williams GJ, Haroon MF, Shibl A and others (2017) Metagenomic covariation along densely sampled environmental gradients in the Red Sea. ISME J 11: 138–151
Throdsen J (2012) The planktonic marine flagellates. In: Tomas CR (ed) Marine phytoplankton: a guide to naked flagellates and coccolithophorids. Academic Press, San Diego, CA, p 7–131
Veldhuis MJW, Kraay GW (1990) Vertical distribution and pigment composition of a picoplanktonic prochlorophyte in the subtropical North Atlantic: a combined study of HPLC-analysis of pigments and flow cytometry. Mar Ecol Prog Ser 68:121–127

Voigt K, Sharma CM, Mitschke J, Joke Lambrecht S, Voß B, Hess WR, Steglich C (2014) Comparative transcriptomics of two environmentally relevant cyanobacteria reveals unexpected transcriptome diversity. ISME J 8:2056–2068

Waldbauer JR, Rodrigue S, Coleman ML, Chisholm SW (2012) Transcriptome and proteome dynamics of a light-dark synchronized bacterial cell cycle. PLOS ONE 7: e43432

Wolf-Vecht A, Paldor N, Brenner S (1992) Hydrographic indications of advection/convection effects in the Gulf of Elat. Deep-Sea Res Part A 39:1393–1401

Yamada T, Letunic I, Okuda S, Kanehisa M, Bork P (2011) iPath2.0: interactive pathway explorer. Nucleic Acids Res 39:W412–W415

Yelton AP, Acinas SG, Sunagawa S, Bork P, Pedrós-Alió C, Chisholm SW (2016) Global genetic capacity for mixotrophy in marine picocyanobacteria. ISME J 10: 2946–2957

Yosef I, Irihimovitch V, Knopf JA, Cohen I and others (2004) RNA binding activity of the ribulose-1,5-bisphosphate carboxylase/oxygenase large subunit from *Chlamydomonas reinhardtii*. J Biol Chem 279: 10148–10156

Zaar A, Gescher J, Eisenreich W, Bacher A, Fuchs G (2004) New enzymes involved in aerobic benzoate metabolism in *Azoarcus evansii*. Mol Microbiol 54:223–238

Editorial responsibility: Zoe Finkel, Sackville, New Brunswick, Canada

Submitted: March 28, 2017; Accepted: August 31, 2017
Proofs received from author(s): November 19, 2017